Exploring Many-Body Dynamics on a Rydberg Quantum Simulator

Johnathan Georgaras
Department of Physics, Stanford University, Stanford, CA 94305
(Dated: June 25, 2020)

Submitted as coursework for PH470, Stanford University, Spring 2020

Computational simulation have their limitations when simulation many-body systems. A physics controllable, coherent many-body systems can provide insights into the quantum many-body dynamics that elude modern computing. The Rydberg, cold-atom array system experimentally realized by Bernien *et al.* in their 2017 paper, "Probing many-body dynamics on a 51-atom quantum simulator" is discussed as one such possible many-body quantum simulators. This Rydberg quantum simulator.

I. INTRODUCTION

Computational approaches serve as the natural domain for many-body quantum experiments in the absence of a fully controlled, coherent many-body quantum system. A classical system such as a computer, however, has its limitations in its applicability and functionality when applied to a quantum system. The goal is therefore to develop a quantum simulator which can provide the same kind of insights into strongly correlated quantum systems for which we currently rely on computers. Such a quantum simulator would allow a better understand of the role of quantum entanglement in the system and allow enable realizations and studies of new states of matter. Bernien *et al.* in their 2017 paper, "Probing many-body dynamics on a 51-atom quantum simulator", suggest an experimental method for creating a deterministically prepared and reconfigurable many-body quantum arrays of individually trapped cold atoms[1]. This review is an overview of their methods and results. All figures and data are qualitatively adapted from those in the original article.

II. BACKGROUND

A. Building a Chain of Strongly Interacting Atoms

Bernien *et al.*'s realization of a quantum simulator involves the coherent coupling of neutral atoms to excited Rydberg states. A Rydberg state occurs when an electron is excited to in a very high, diffuse orbital which interacts only weakly with other electrons in the atom[2]. This separation creates a strong dipole resulting in repulsive van der Waals interactions (of strength $V_{ij} = C/R_{ij}$) between Rydberg atom pairs (separated by distance R_{ij}). Fig. 1a describes how the cold neutral Rubidium atoms are arranged as an array in the simulator. Individual Rubidium atoms (green) are trapped using optical tweezers (vertical red beams) and arranged into 1-D chains. The lateral black arrows represent the coherent van der Waals interactions V_{ij} between excited atoms. Atoms are excited by the horizontal red and blue beams to a Rydberg state with strength Ω and detuning Δ. The quantum dynamics of this constructed system are governed by the system Hamiltonian

$$\frac{\mathcal{H}}{\hbar} = \sum_i \frac{\Omega_i}{2}\sigma_x^i - \sum_i \Delta_i n_i + \sum_{i<j} V_{ij} n_i n_j \qquad (1)$$

where Δ_i are the detunings of the driving lasers from the Rydberg state, $\sigma_x^i = |g_i\rangle\langle r_i| + |r_i\rangle\langle g_i|$ is the coupling between the ground state $|g_i\rangle$ and the Rydberg state $|r_i\rangle$ of an atom at position i in the chain driven at a Rabi frequency Ω_i, $n_i = |r_i\rangle\langle r_i|$, and $\hbar$ is the reduced Planck constant. Here, homogenous coherent coupling is used ($|\Omega_i| = \Omega$, $|\Delta_i| = \Delta$), which is controlled by changing lasers intensities and detunings in time. The interaction strength V_{ij} is tuned either by varying the distance between atoms or by coupling atoms to different Rydberg states.

Fig. 1b shows the two-photon process which couples the ground state $|g\rangle$ to the Rydberg state $|r\rangle$. The two laser frequencies can be controlled to select the desired detuning Δ. By the experimental protocol, atoms are loaded from a laser-cooled cloud of Rubidium-87 atoms in a magneto-optical trap (MOT) into the array of tweezers[3]. Tweezers are filled probabilistically with an average single-atom loading probability of $p \approx 0.6$. Occupied and empty tweezers are distinguished using fluorescence imaging. Unoccupied traps are switched off and the remaining occupied tweezers are moved to the left until they stack up with a desired spacing. This process eliminates entropy associated with the probabilistic loading in a similar idea to "Maxwell's demon"[4]. The single-atom occupation probability in the left-most

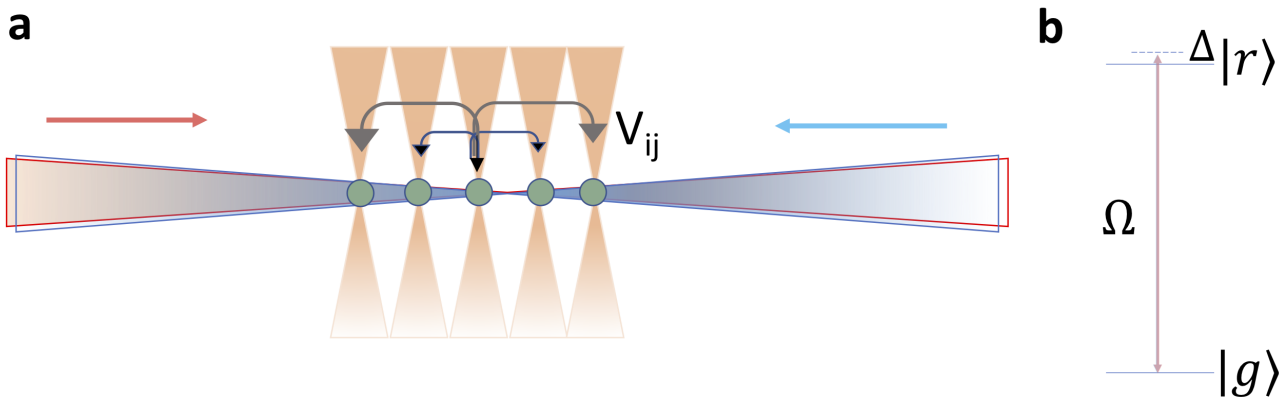

FIG. 1: **Experimental Platform. a**, Rubidium atoms (green) are trapped using optical tweezers (vertical red beams) and arranged in to defect-free array. Rydberg states are coupled with strength Ω and detuning Δ (inset). **b**, A two-photon process coupling the ground state $|g\rangle$ to the excited Rydberg state $|r\rangle$. Driving lasers at frequencies Ω are detuned to get are an overall detuning of Δ. Figure and data adapted from Bernien *et al.*[1] (Source: J. Georgaras, after Bernien et al. [1])

traps increases from $\approx$ 0.6 before rearrangement to 0.988(3) after rearrangement, demonstrating the ability for high-fidelity single-atom preparation.

These occupying atoms are prepared in a well-defined internal ground state $|g\rangle$. The traps are turned off and the system evolves under unitary time evolution $U(\Omega, \Delta, t)$ by the use of laser light coupling. This evolution can be implemented in parallel on several non-interacting subsystems. The traps are then turned back on and the ground state atoms remain and the excited atoms are ejected from the trap. Fluorescence imaging distinguishes occupying ground state atoms and the now unoccupied "holes" left by the excited states. This is known as the "Rydberg blockade". Multiple Rydberg excitations are suppressed when two atoms are close enough such that their Rydberg induced van der Waals interactions V_{ij} exceed the Rabi frequency Ω. The Rydberg blockade radius R_b is the separation of atoms such that $V_{ij} = \Omega$. As multiple atoms are brought close to each other, the dynamics change as one excitation is effectively shared between atoms in clusters of size N. Rabi oscillations between the ground state and a collective state with exactly one excitation ($W = 1/\sqrt{(}N)\ldots$) have a frequency which scales as $\sqrt{(}N)$. These observations enable the coherence properties of the system to be quantified.

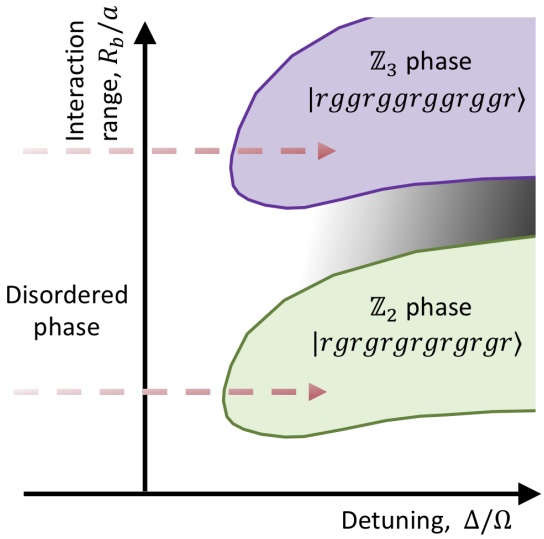

FIG. 2: **Phase diagram and build-up of crystalline phase.** A qualitative schematic of the ground-state phase diagram of the Hamiltonian in equation (1). Different possible broken symmetry phases are shown. These different phases are dependent on interaction range R_b/a (R_b, blockade radius; a, trap spacing) and detuning Δ (see main text). Figure and data adapted from Bernien *et al.*[1] (Source: J. Georgaras, after Bernien et al. [1])

B. Encoding the Quantum Simulator

Once prepared, the quantum system created by the array of Rydberg atoms begins to resemble the paradigmatic Ising chain of spin-1/2 particles. The system Hamiltonian equation (1) can be compared to that of the paradigmatic Ising model in an external magnetic field for effective spin-1/2 particles with the Rydberg and the ground states being equivalent to the spin-up and spin-down states. Additionally, the magnetic interaction between atoms in the Ising model is simulated by the Rydberg interactions. As such, this system provides a powerful foundation for exploring a rich variety of many-body physics as a

quantum simulator. One theoretical avenue to probing is that of its ground state. The lowest ground energy state of the quantum simulator displays many phases, each with various broken symmetries depending on the interaction range R_b/a (R_b, blockade radius; a, trap spacing) and preparation detuning Δ. The shaded areas illustrated in Fig. 2 indicate incommensurate regions each representing a different phase.

At large negative ratio of Δ/Ω, the ground state corresponds to the disordered, paramagnetic phase where all atoms are in the state $|g\rangle$. However, as Δ/Ω increases to large positive values, the number of Rydberg atoms $|r\rangle$ increases (conceptualized in the Hamiltonian as the number operator coefficient Δ now outweighing the coupling coefficient Ω) and the interaction between excited atoms is no longer negligible. These interactions generate the spatially ordered phases, called "Rydberg crystals" with the different spatial symmetries, illustrated in Fig. 2. These phases correspond to the relative strength of the Rydberg interactions to the detuning-Rabi ratio (recall Rydberg interaction strength dependent on atom spacing). If $V_{i,i+1} \gg \Delta \gg \Omega \gg V_{i,i+2}$, that is, the nearest-neighbor interaction outweighs the detuning-Rabi ratio but next-nearest neighbor interaction does not, then we get the a clustering (seen before with the Rydberg blockade) of size two. In this case, the ground state breaks $\mathbb{Z}_2$ translational symmetry (the "alternating pattern" phase shown in Fig. 2) similar to the antiferromagnetic order in the Ising chain. The interaction strength V_{ij} can be further extended to further neighbors, thus creating larger cluster blockades, and a higher degree broken translational symmetries is obtained along the chain.

The performance of this quantum simulator can be benchmarked by comparing the measurement of the $\mathbb{Z}_2$ phase order with the theoretical predictions in an $N = 7$ atom system. Fig. 3a illustrates the experimental procedure graphically. A driving laser shoots a square-shaped pulse $\Omega(t)$ (blue) while slowly changing detuning $\Delta(t)$ (red) from negative to positive values. Fig. 3b shows how the system excitation probabilities evolves over time while the driving laser is on. The data points are obtained by varying the stopping time t_{stop} of the laser excitation pulse and state of the system is read. The $\mathbb{Z}_2$ order phase eventual become the most probable, as illustrated in Fig. 3c. When corrected for known detection infidelity, the desired many-body state is reported to be reached experimentally with a probability $P = 77(6)\%$.

The preparation fidelity of the quantum simulator is found to be dependent on array size. The probability of observing the system in the many-body ground state at the end of the sweep was found to decrease was the system size decreases. As per the name of the paper, systems even as large as 51 atoms were found to produce a perfectly ordered crystalline many-body ground state with a probability of $P = 0.9(2)\%$ when corrected for detection fidelity). This result is especially remarkable because the Hilbert space grows exponentially with atoms. A system with 51 atoms has a Hilbert space of dimension 2^{51} and it was found that a state with perfect $\mathbb{Z}_2$ order is the commonly observed many-body state given the appropriate spacing over 18,349 experimental realizations[1].

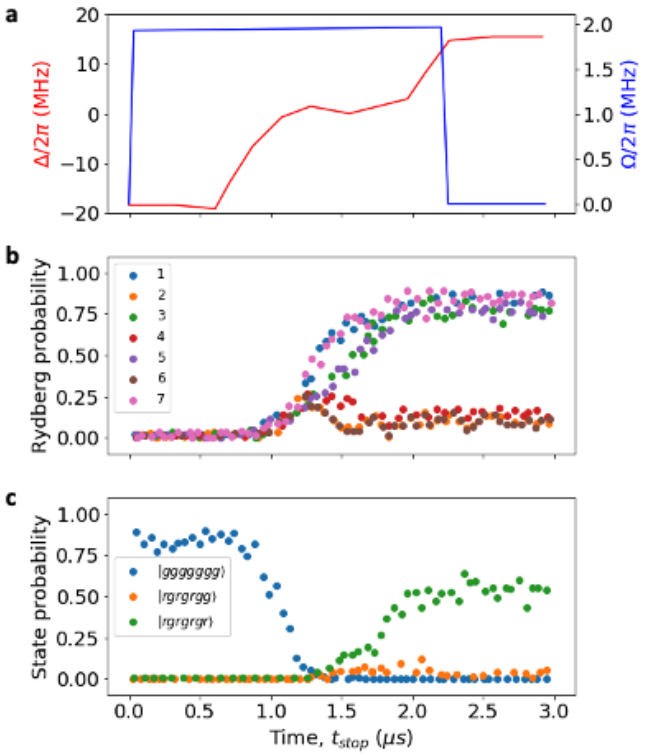

FIG. 3: **Comparison with a fully coherent simulation.** **a**, Frequency of the driving laser over time. A square-shaped pulse $\Omega(t)$ (blue) is sent with detuning from negative $\Delta(t)$ (red) to positive. b, Rydberg excitation probability for atoms in a 7-atom cluster (colored points), measured at various stopping times of the laser pulse $\Omega(t)$. Experimentally performed by Bernien *et al.*[1]. **c**, Evolution of the seven most probable many-body states. Target reached with probability 77(6)% when corrected for finite detection fidelity. Figure and data adapted from Bernien *et al.*[1] (Source: J. Georgaras, after Bernien et al. [1])

C. Observing Many-Body Quantum Dynamics Across a Phase transition

Now, with a 51-atom quantum simulator in hand, the many-body dynamics can be studied across the phase transition into the $\mathbb{Z}_2$ region. A slow sweep of the laser detuning across resonance, as described previously, is illustrated in Fig. 4. Long, ordered chains are observed with atomic states that alternate between the Ry-

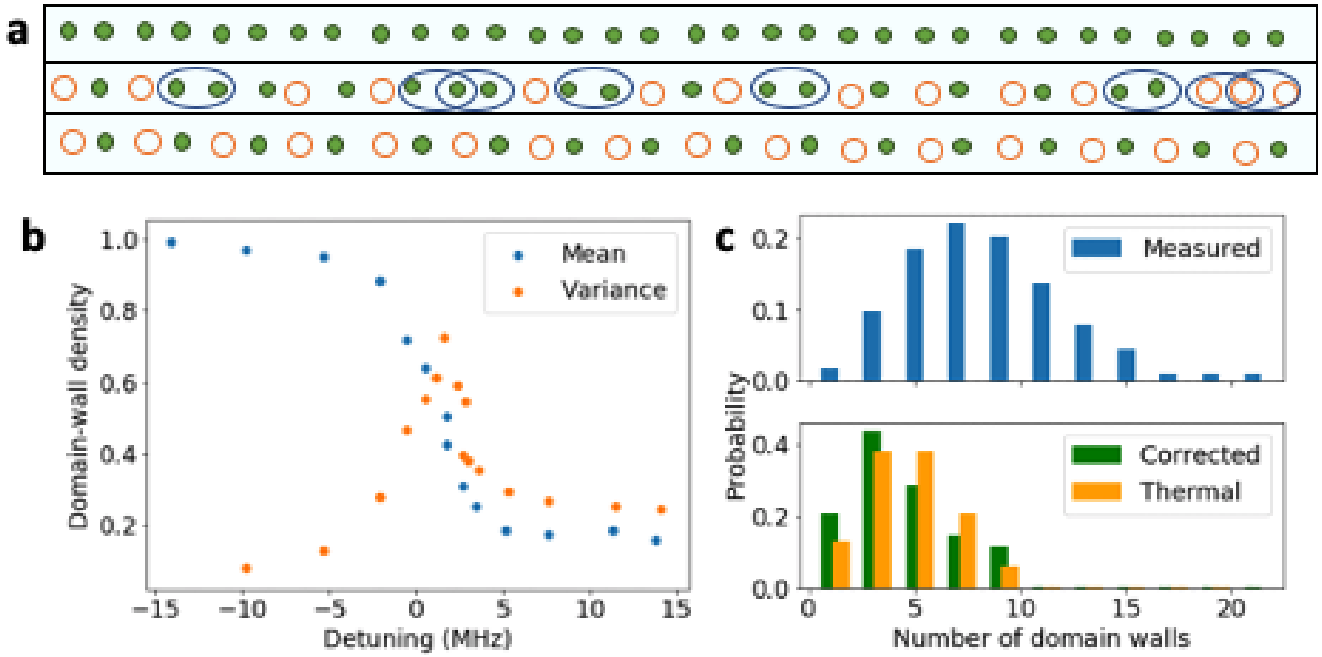

FIG. 4: **Quantifying $\mathbb{Z}_2$ order in a 51-atom array after a slow detuning sweep. a**, Schematic representation of a slow detuning sweep realization. Domain walls shown as blue circles. **b**, The mean domain-wall density (blue) decreases along the detuning sweep and indicates the onset of phase transition. Variance in domain-wall density (red) peaks at transition point. **c**, domain-wall distribution measured by Bernien *et al.* over 18,439 experimental realizations (blue). Green points indicates the finite detection fidelity correction: average of 5.4 domain walls. This is compared with the distribution that would come from a thermal state with the same mean domain-wall density. Figure and data adapted from Bernien *et al.*[1] (Source: J. Georgaras, after Bernien et al. [1])

dberg and ground states. This pattern, however, does not continue along the entire 51-atom chain. Many ordered domains are seen in the single-shot fluorescence images of Fig. 4a. These domains are separated by domain walls that consist of two neighboring atoms in the same electronic state (either Rydberg-Rydberg, or ground-ground). The number of domain walls in the 51-atom system can be considered as a quantification of the transition from the disordered phase to the ordered $\mathbb{Z}_2$ phase as a function of detuning Δ. The number of ordered domains increases as the system enters the $\mathbb{Z}_2$ phase and so the number of domain-walls decreases (Fig. 4b). While the mean number of domain-walls decrease over each of the experimental realizations, the decrease is not consistent and so the variance of domain-wall density peaks at the transition point. A variance peak at the transition point is in agreement with expectations for an Ising-type second-order quantum phase transition[5]. The measured position of this peak is $\Delta \approx 0.5\Omega$. In the large detuning limit, $\Delta \gg \Omega$, and the Ω term in the Hamiltonian equation (1) can be neglected. An effectively classical Hamiltonian emerges

$$\frac{\mathcal{H}_{cl}}{\hbar} = -\Delta \sum_{i=1}^{N} n_i + \sum_{i=1}^{N-1} V_1 n_i n_{i+1} + \sum_{i=1}^{N-2} V_2 n_i n_{i+2} \quad (2)$$

The eigenstates of this Hamiltonian are the 2^N classical configurations of each atom either in $|g\rangle$ or $|r\rangle$. Only the next-nearest neighbor interactions are considered because the coupling strengths for longer distances are weak compared to the maximum timescale accessible by the experiment. Deep in the $\mathbb{Z}_2$ phase, this classical regime enables the direct inference of excitation statistics from the measured domain-wall number. The number of domain walls in this regime as measured are depicted in Fig. 4c to have an average of 9.01(2). Corrections for detection fidelity using maximum-likelihood estimation[1] gives a distribution corresponding to a state that has on average 5.4 domain walls. A perfect $\mathbb{Z}_2$ ordered phase, however, should have no domain walls as no two neighboring atoms would share electronic states. Bernien *et al.* assume that the appearance of domain-walls here come from non-adiabatic transitions from the ground state at the phase transition[1].

The $\mathbb{Z}_2$-ordered phase that is created can be further characterized by a correlation function between positions

$$g_{ij}^{(2)} = \langle n_i n_j \rangle - \langle n_i \rangle \langle n_j \rangle \quad (3)$$

where $\langle \dots \rangle$ is the average over experimental repetitions. The position correlations are found to decay expo-

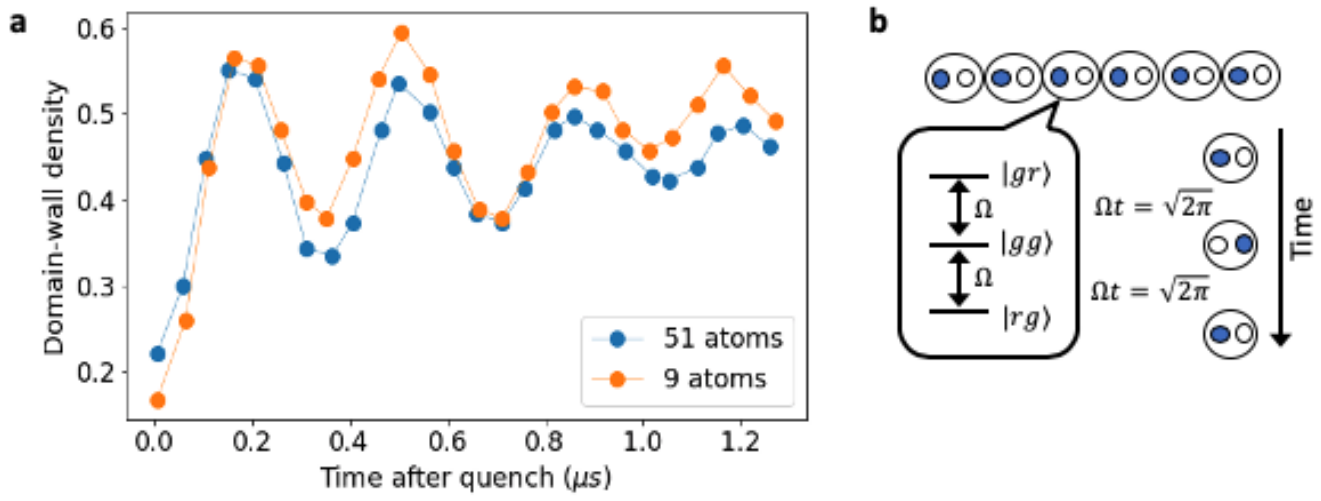

FIG. 5: **Emergent oscillations in many-body dynamics after sudden quench. a**, Domain-wall density as a function of time after the quench. Oscillations decay at a timescale of $0.88\mu s$. **b**, Model of non-interacting dimers made of a ground state atom (blue) and Rydberg atom (white). Figure and data adapted from Bernien *et al.*[1] (Source: J. Georgaras, after Bernien et al. [1])

nentially over distance with a decay length of $\xi = 3.03(6)$ sites (further discussed in the next section).

D. Quenching Dynamics of an Ordered Phase

Beyond exploring phase transitions, the quantum simulator also enables the study of many-body dynamics far from equilibrium. Bernien *et al.* focus on the quench dynamics of a Rydberg crystal initially prepared in the effectively classical, deep $\mathbb{Z}_2$-ordered phase. The "quench" procedure consists of adiabatically preparing a $\mathbb{Z}_2$-ordered system (i.e. large detuning Δ/Ω as explained above) and then changing the detuning $\Delta(t)$ suddenly to the single-atom resonance ($\Delta = 0$). After the quench, oscillations between the initial crystal and it's complimentary crystal (i.e. every atomic state in each position is inverted, $|r\rangle \to |g\rangle$ and $|g\rangle \to |r\rangle$) are observed. These oscillations are observed to be robust and persist over several periods with a frequency independent of system size. These oscillations are measured by the domain-wall density function over time (Fig. 5a). The domain-wall density oscillation is at a minimum when the system is in a $\mathbb{Z}_2$-ordered state, and a maximum when the state has disappeared while flipping to its compliment. The initial crystal is found to revive with a period that is slower by a factor of 1.38(1) compared to[1] Rabi-oscillation for independent, non-interacting atoms. It is striking that there are coherent and persistent oscillations of the crystal because with respect to the quenched Hamiltonian ($\Delta = 0$), the energy density of the $\mathbb{Z}_2$-ordered state corresponds to that of infinite temperature ensemble[1]. Also, while the Hamiltonian does not have any explicitly conserved quantities (other than total energy), the oscillations nevertheless persist at periods larger than the natural timescales of local relaxation ($1/\Omega$; emission) and the fastest timescale ($1/V_{i,i+1}$; decoherence).

Furthermore, Bernien *et al.* show that that $\mathbb{Z}_2$-ordered state cannot be characterized by a simple thermal ensemble[1]. In the deep, $\mathbb{Z}_2$-ordered phase where we get the effectively classical regime, the classical thermal ensemble can be represented as $\rho = exp(-\beta\mathcal{H}_c l)/Z$, with $Z \equiv tr[exp(-\beta\mathcal{H}_c l)]$ and inverse temperature β. The probability of finding a particular configuration i is $p_i = exp(-\beta E_i)/Z$. The correlation function can be determined from the characterized inverse temperature β of a system which matches the experimentally determined average domain-wall density. Bernien et al find that the correlation length in the corresponding thermal state is $\xi_{th} = 4.48(3)$, which is longer than the measured correlation length $\xi = 3.03(6)$. The experimentally prepared state is therefore not classically thermal, suggesting that the system does not thermalize within the timescale of $\mathbb{Z}_2$.

III. DISCUSSION

A full explanation of these observed oscillations, or "many-body revivals", are still lacking. Many-body revivals repeatedly return to their initial state and fail to thermalize *irrespective* of their prepared initial state. The inconsistencies with ergodicity and thermalization of the experimental results have spurred research into so-called "many-body quantum scars" to explain the oscillations.[6] At the time of writing, Bernien *et*

al. proposed a simplified model to understand these observations[1]. First, assume the effect of long-range interactions is neglected; and second, that nearest-neighbor interactions are replaced by a constraint on neighboring excited Rydberg states. With these assumptions, the behaviour of the quench dynamics can be modelled by dimerized spins, as illustrated in Fig 5b. The Rydberg blockade constrains each dimer into an effective spin-1 system with three states ($|rg\rangle$, $|gg\rangle$ and $|gr\rangle$). Fig. 5b demonstrates how the resonant drive 'rotates' the three states over the period $\sqrt{2}(2\pi/\Omega)$, which is closer to what is observed experimentally.

Using a time-dependent variational principle, Bernien *et al.* derive analytical equations of motion for the many-body wave function based on matrix product states on all blockade constraints (even though this dimer model neglects interactions between dimers). An oscillation with a frequency of about $\Omega/1.51$ is found and matches various numerical simulations[1]. This model could be further enhanced by the addition of long-range interactions and the system is observed to decay at a faster timescale ($1/V_{i,i+2}$) which better matches experimental observations of entropy. The observations by Bernien *et al.* indicate that the decay of crystal observations is governed by weak next-nearest-neighbor interactions and the system decays much slower relative to a thermal model. This is unexpected as the Hamiltonian is far from an integrable system and shows neither strong disorder nor explicitly conserved quantities, which would suggest it should thermalize more easily. The dimer model provides a better approximation for these observations at this point.

IV. CONCLUSION

Bernien *et al.* demonstrated that a Rydberg excitation of arrays of neutral atoms is a promising simulator of many-body quantum dynamics in large systems. These methods can be extended and improved in many ways including: qubit rotations about different axes to get spin-orbit effects; implementing a 2D array to get very large systems; and better controllability by using state-selective Rydberg excitation along hyperfine sublevels. These extensions would allow the exploration and probing of new many-body phenomena in quantum dynamics. These include many-body coherence and entanglement, exploring stable non-equilibrium phases, many-body scars, and the interplay between long-range interactions and disorder. Finally, it should be noted that this approach is also well suited for the physical realization and testing of quantum optimization algorithms with systems sizes that are unfeasible for classical computers.

[1] Bernien, H., et al., "Probing many-body dynamics on a 51-atom quantum simulator" Nature **551.7682** (2017).

[2] Roos, B. O. , "Perspectives in calculations on excited state in molecular systems" Computational Photochemistry (2005).

[3] Endres, M., et al., "Atom-by-atom assembly of defect-free one-dimensional cold atom arrays" Science **354(6315)** (2016).

[4] Knott, C. G., "Quote from undated letter from Maxwell to Tait" Life and Scientific Work of Peter Guthrie Tait (1911).

[5] Sachdev, S., Quantum Phase Transitions 2nd Edn. (2009).

[6] Turner, C. J., et al., "Quantum scarred eigenstates in a Rydberg atom chain: Entanglement, breakdown of thermalization, and stability to perturbations." Physical Review B **98.15** (2018).